EPJ Web of Conferences **233**, 05008 (2020) https://doi.org/10.1051/epjconf/202023305008
CMPNC 2019

Simulation of the temperature profile of $BaCaZrTiO_3$ thin films during laser annealing

Tiago Rebelo[1,*], *João* Alves[1], and *Bernardo* Almeida[1]

[1]Centre of Physics/Department of Physics, University of Minho, Gualtar Campus, Braga, Portugal

Abstract. The laser annealing of a $Ba_{0.85}Ca_{0.15}Ti_{0.9}Zr_{0.1}O_3$ (BCZT) thin film on a metglas substrate was simulated in order to understand how the annealing parameters (energy and fluence of the laser, pulse duration, etc) influence the optimization of the crystallinity of the film. Using a 1D heat diffusion equation combined with a finite difference method, the variation of the temperature with the depth relative to the film's surface and on annealing time was studied. The laser intensity, BCZT's reflectivity and the temperature dependence of the thermal conductivity and specific heat of the BCZT were considered. No structural phase changes were detected in both the BCZT and the metglas for the values of laser fluence studied, but for 80 mJ/cm^2 the maximum temperature approached near the BCZT's melting temperature. It was observed that since the film's thermal conductivity decreases with increasing fluence, lower fluences allow for a better distribution of the laser's energy throughout the crystal lattice, increasing the crystallinity. It was further observed that between consecutive pulses the film's temperature stabilizes at room temperature.

1 Introduction

Multiferroic piezoelectric-magnetostrictive composites have been attracting much attention, since they allow exploring coupled electric/magnetic responses [1, 2]. Composite nanostructures made of $Ba_{0.85}Ca_{0.15}Ti_{0.9}Zr_{0.1}O_3$ (BCZT, ferroelectric) thin films on Metglas 2826MB (ferromagnetic) substrates are one of such composites, combining the high piezoelectricity of the BCZT with the high magnetostriction of the metglas, originating a multiferroic material with potential enhanced coupled responses. However, when producing the thin film, high deposition temperatures may be required [2] that modify the substrate properties. In such cases a possible approach is to perform the deposition at low temperatures followed by an annealing process using a laser with a low fluence (*laser annealing*), which will remove defects that may have accumulated during the deposition, promote the film crystallization and avoid heating the substrate [3]. This annealing process is particularly indicated when the materials involved can't withstand the temperatures reached in a conventional annealing in an oven, as is the case with the materials used in this work: the metglas substrate has an irreversible structural phase change (crystallization) at 450 °C that degrades its magnetic properties, while the BCZT film requires a deposition temperature of approximately 700 °C. By depositing the BCZT layer at 400 °C over the metglas substrate and subsequently laser annealing the film, the crystallization of the BCZT layer can be achieved without affecting

*e-mail: rebelo.tiago@gmail.com

the metglas' properties. There is then interest in studying how the film's temperature varies during this process, both with the depth relative to its surface and with time, as it allows the optimization of the annealing conditions (laser energy and fluence, pulse duration, etc). To this end, the variation of the laser pulse intensity with time and the temperature dependence of the specific heat and thermal conductivity have to be considered. The effect of the temperature on the substrate is also of interest. It was observed that the laser does not contribute appreciably to its heating, as envisaged. The main effect of the substrate in the composite is the absorption of energy from the film and, consequently, the lowering of its temperature.

Given the similarity between BCZT and barium titanate ($BaTiO_3$), its base compound, the properties of the later can be used instead of those of the former in the calculations. This was done during this study whenever the desired BCZT properties could not be found.

2 Experimental procedure

Given that the focus of this work is the modeling of the temperature profile during the laser annealing, only a brief description will be given reagarding the film growth technique. More detailed descriptions can be found in [4, 5]. The film was grown via pulsed laser ablation with a KrF Lambda Physik LPXPro 210 laser with wavelength $\lambda = 248$ nm and a pulse duration of 18 nanoseconds (FWHM). The same laser was used in the laser annealing procedure. The BCZT film was deposited at 400 °C under an oxygen atmosphere, with a pressure of 0.02 mbar, and a fluence of 2 J/cm^2. To perform the laser annealing process, the film was struck with the same laser but using a lower energy than that used during the deposition. Also, the beam was defocused to reduce the fluence. A frequency of 10 Hz was used and 3 values of laser fluence were studied: 40, 50 and 80 mJ/cm^2. The annealing process was performed during 200 seconds in air, to preserve the film's oxidation level. Figure 1 shows the experimental apparatus for the procedure.

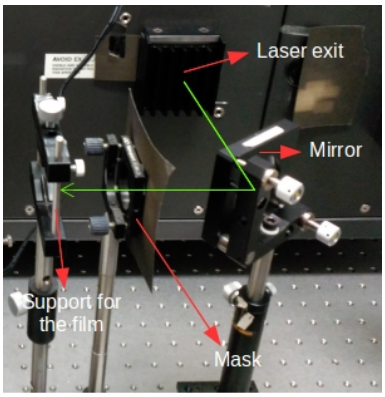

Figure 1. Experimental apparatus for the laser annealing process. The laser path is shown in green.

3 Heat diffusion in the samples

The geometry of the film, as well as its positioning relative to the laser during the annealing process, allow the heat diffusion to be well described by the 1D Fourier heat diffusion equation [3]:

$$\rho_f C_P \frac{\partial T(x,t)}{\partial t} - \frac{\partial}{\partial x}\left[k\frac{\partial T(x,t)}{\partial x}\right] = P(x,t) \tag{1}$$

where $T(x,t)$ is the temperature at depth x relative to the film's surface and at time t, ρ_f is the density of the film [6], C_P and k are its specific heat and thermal conductivity respectively, and $P(x,t)$ is the heat generation function, a function that models the effect of the heat source - in this case, the laser. However, when C_P and k vary strongly with temperature, as in our laser heated samples, equation 1 can't be directly used to obtain an analytical solution [3].

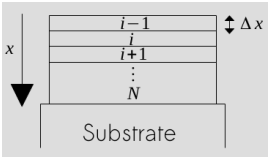

Figure 2. Division of the film in several layers of equal thickness during the discretization procedure.

An alternative is to discretize the problem: the film is divided in several layers of equal thickness (Figure 2) originating an equation for each layer.

We can then obtain the temperature of each layer, i, at the next instant $(n+1)$ based on the temperature of that layer at the previous instant (n), as well as the temperatures and thermal conductivities of the adjacent layers at the previous instant (equation 2). The substrate can be included in the model by considering it as an extension of the film and applying the discretization procedure. In the film-substrate interface, however, the density, thermal conductivity and specific heat of the metglas have to be considered.

$$T_i^{n+1} = T_i^n + \frac{\Delta t}{\rho_f C_{P_i}^n} P(x,t) + \frac{\Delta}{\Delta x^2} \frac{1}{\rho_f C_{P_i}^n} \left[k_{i-1}^n \left(T_{i-1}^n - T_i^n \right) + k_{i+1}^n \left(T_{i+1}^n - T_i^n \right) \right] \tag{2}$$

We also need boundary conditions. The chosen conditions were: 1) there is no heat loss through the surface [3], which means that the surface layer is at the same temperature as the atmosphere immediately in contact with it - $T_0^n = T_{-1}^n$; 2) the sample is thick enough for the temperature to stabilize with increasing distance from the surface, which means that the final layer of the substrate (layer N) is in thermal equilibrium with the following layer - $T_N^n = T_{N+1}^n$. The following layer would be the sample support, which is at room temperature, so this boundary condition is simply $T_{N+1}^n = 293.15$ K. Applying these conditions to equation 2 we obtain a set of equations for each layer of the film and substrate:

$i = 0$:

$$T_i^{n+1} = T_i^n + \frac{\Delta t}{\rho_i C_{P_i}^n} P_i(x,t) + \frac{\Delta t}{\Delta x^2} \frac{1}{\rho_i C_{P_i}^n} k_{i+1}^n \left(T_1^n - T_0^n \right) \tag{3}$$

$i = 1, ..., N-1$:

$$T_i^{n+1} = T_i^n + \frac{\Delta t}{\rho_i C_{P_i}^n} P_i(x,t) + \frac{\Delta t}{\Delta x^2} \frac{1}{\rho_i C_{P_i}^n} \left[k_{i-1}^n \left(T_{i-1}^n - T_i^n \right) + k_{i+1}^n \left(T_{i+1}^n - T_i^n \right) \right] \tag{4}$$

$i = N$:

$$T_i^{n+1} = T_i^n + \frac{\Delta t}{\rho_m C_{P_m}} P_m(x,t) + \frac{\Delta t}{\Delta x^2} \frac{1}{\rho_m C_{P_m}} k_m \left[\left(T_{i-1}^n - T_i^n \right) + \left(293.15 - T_i^n \right) \right] \tag{5}$$

where ρ_i, C_{P_i} and $P_i(x,t)$ are, respectively, the density, specific heat and heat generation function of the material that constitutes the ith layer, and ρ_m, C_{P_m}, k_m and $P_m(x,t)$ are, respectively, the density [7], specific heat ([8], refering to Metglas 2605S-2, but expected to be similar), thermal conductivity [9] and heat generation function of the metglas. The values of the ith layer's physical properties correspond to either BCZT or metglas, depending on the position.

Finally, for the simulations performed, a film thickness of approximately 500 nm and substrate thickness of 10 μm were chosen as reasonable values, in accordance with the scanning electron microscopy studies performed on the samples. After some experimentation, the time step $\Delta t = 1$ ns and layer thickness $\Delta x = 65$ nm were chosen as the smallest representative values that the computational resources available could handle.

The heat generation function is of the form $P(x,t) = C(1-R)I(t)\exp(-\alpha x)$, where C is a normalization constant, R and α are, respectively, the reflectivity and absorption coefficient of the BCZT, $I(t)$ is the time dependent laser profile pulse intensity and x is the depth relative to the film's surface. The reflectivity of the BCZT can be determined considering that the laser light is unpolarized and using barium titanate's refractive index ([10], $\lambda = 244.3$ nm).

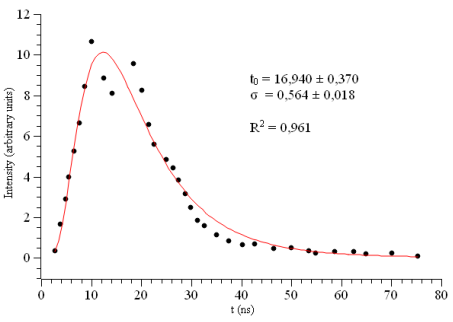

Figure 3. Fitting of the laper profile with a lognormal dependence on time. t_0 is related to the instant at which $I(t)$ is maximum and σ is the standard deviation. R^2 is the statistical measure of goodness of fit.

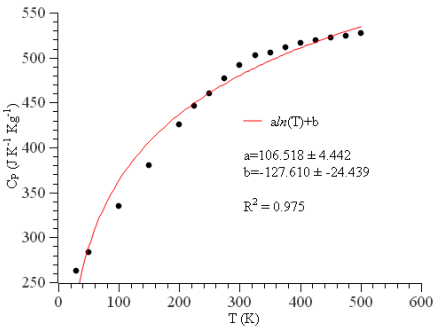

Figure 4. The specific heat follows reasonably well a logarithmic dependence on the temperature (data from [11].

The absorption coefficient is related to λ and to the extinction coefficient of the BCZT (taken from [10], for $BaTiO_3$). In regard to $I(t)$, the laser profile was obtained from the manufacturer and it was fitted (Figure 3) with a lognormal function. It is observed that $I(t) \approx 0$ from 50 ns onwards. So, this value was taken as the pulse duration, τ. Attending to the normalization condition for $P(x,t)$, $C = F_0/\tau$, where F_0 is the fluence of the laser, we finally obtain the heat generation function for the BCZT:

$$P(x,t) = (1-R)\frac{F_0}{\tau}\frac{1}{(t/t_0)\sigma\sqrt{2\pi}}\exp\left(\frac{-\ln^2(t/t_0)}{2\sigma^2}\right)e^{-\alpha x} \tag{6}$$

The used t_0 and σ values are in Figure 3. The heat generation function for the substrate depends on the amount of laser radiation that reaches its surface layer, that is, it depends on the value of $P(x,t)$ at the final layer of the BCZT. Our calculations show that this value is < 0.05 W m^{-3}, so we conclude that $P_m(x,t) \approx 0$. Consequently, the second term on the right hand side of equations 4 and 5 becomes negligible in the substrate case and was dropped from its calculations.

The temperature dependence for the BCZT's specific heat, $C_P(T)$, was obtained by fitting a curve to experimental data (Figure 2(b) of [11]). A logarithmic dependence on temperature was fitted (Figure 4). This is reasonable from a physical point of view, as it is expected that $C_P \to$ constant as $T \to \infty$.

For the temperature dependence of the thermal conductivity, $k(T)$, there is indication [12] that, for $BaTiO_3$, it decreases with increasing temperature more slowly than $k \propto T^{-1}$ in the temperature range here considered. The expected dependence will thus be of the form:

$$k(T) = \frac{A}{T^\beta}, \quad \beta < 1 \tag{7}$$

where A and β are constants determined by attending to the boundary conditions given in [12], $k(T) = 2.51$ W m^{-1}K^{-1} for $T = 1000$ K and $k(T) = 4.99$ W m^{-1}K^{-1} for $T = 300$ K, but adapting the second boundary condition to the fact of the BCZT being a ceramic, so that $k(300) = 2.85$ W m^{-1}K^{-1} [6]. This resulted in $A \approx 73.9$ W m^{-1} and $\beta \approx 0.571$.

4 Results

The temperature profiles $T(x,t)$ for the different values of laser fluence studied (40, 50 and 80 mJ/cm^2) are presented in Figures 5, 6 and 7. Only the layers of the substrate that exhibited some heating are shown.

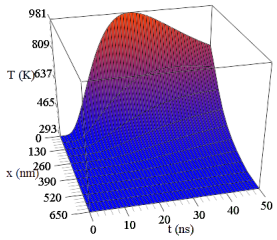

Figure 5. Temperature profile $T(x,t)$ for $F_0 = 40$ mJ/cm^2.

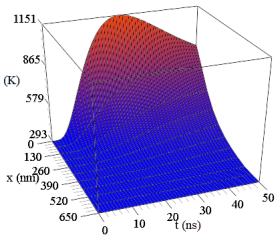

Figure 6. Temperature profile $T(x,t)$ for $F_0 = 50$ mJ/cm^2.

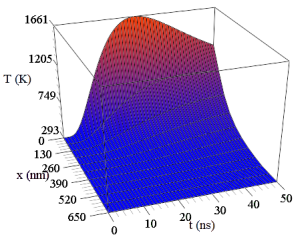

Figure 7. Temperature profile $T(x,t)$ for $F_0 = 80$ mJ/cm^2.

As expected, an increase in laser fluence increases the reached temperatures, but no melting of the BCZT is observed ($BaTiO_3$ melting temperature: ≈1898 K [13]). The temperatures reached in the highest fluence studied, however, approach the melting temperature, but only on the most superficial layer of the BCZT. This is expected from the behaviour $k \propto T^{-1}$ of the thermal conductivity. As the temperature rises due to higher fluences, k will decrease in the considered temperature range, which means that the laser energy won't be as easily transmitted to the inner layers of the film. This leads to an accumulation of energy on the superficial layer and considerable increase of its temperature in comparison with the rest of the film. As such, lower fluences may be more desirable during the annealing process, as they will generate lower temperatures and, consequently, won't decrease the thermal conductivity. This will promote the propagation of the laser energy to the inner layers of the film, originating a more uniform distribution of the energy and promoting the film crystallinity, the intended goal of the annealing process.

Regarding the substrate, it was observed that only its most superficial layers experience some small heating. However, there is interest in stuying how the temperature evolves between consecutive pulses, since the propagation of energy to the substrate may increase the temperature further during this interval. Since each pulse has an effective duration $\tau = 50$ ns and the laser frequency is 10 Hz, the time between consecutive pulses is about 10^8 ns.

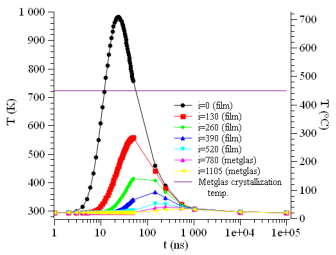

Figure 8. Temperature profile $T(t)$ for $F_0 = 40$ mJ/cm^2.

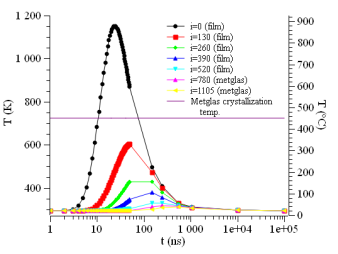

Figure 9. Temperature profile $T(t)$ for $F_0 = 50$ mJ/cm^2.

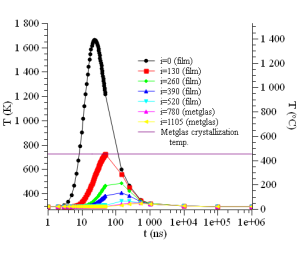

Figure 10. Temperature profile $T(t)$ for $F_0 = 80$ mJ/cm^2.

Figures 8, 9 and 10 show the simulations of the variation of the temperature with time, $T(t)$, for several reference layers in both film and substrate. The metglas' crystallization temperature is also represented (pink horizontal line). No fluence induces crystallization in the metglas. It is also observed that all layers, both from the BCZT and the metglas, stabilize at room temperature before the beginning of the next pulse, independently of the fluence. As such, from a thermal viewpoint the situation is the same in each pulse, always reaching the same level of heating in each layer. This suggests that an extension of the laser pulse in time, in such a way that between consecutive pulses no temperature stabilization occurs (but without provoking crystallization of the metglas), would allow for energy accumulation in the film. This, combined with a low laser fluence, would provide an uniform energy distribution throughout the crystal lattice, optimizing the film crystallinity without affecting the metglas.

5 Conclusions

We developed a model to simulate the temperature profile $T(x,t)$ of BCZT thin films on metglas substrates, during a laser annealing process. The model involved the construction of a heat generation function (describing the effect of the laser on the sample), as well as taking into account the temperature dependence for the specific heat and the thermal conductivity. The temperature profiles obtained revealed that no melting of the BCZT occurs for any of the fluences studied. Further, it revealed that the thermal conductivity plays a relevant role in the temperatures achieved and layers affected by the heating, indicating that lower fluences may be more desirable to promote the uniform distribution of energy throughout the crystal lattice and, consequently, the crystallinity of the film. It was observed that the metglas doesn't experience significant heating, as envisaged, and that between consecutive pulses the temperature of both film and substrate stabilizes at room temperature.

References

[1] N.A. Spaldin & R. Ramesh, Nature Materials **18**, 203-212 (2019)

[2] J.G. Barbosa, I.T. Gomes, M.R. Pereira, C. Moura, J.A. Mendes and B.G. Almeida, J. Appl. Phys. **116**, 164112 (2014)

[3] R.F. Wood & G.E. Giles, Physical Review B **23**, 2923-2942 (1981)

[4] C. Araújo, B.G. Almeida, M. Aguiar, J.A. Mendes, Vacuum **82**, 1437-1440 (2008)

[5] I.T. Gomes, B.G. Almeida, A.M.L. Lopes, J.P. Araújo, J. Barbosa, J.A. Mendes, J. Magn. Magn Mater. **322**, 1174-1177 (2010)

[6] Yi He, Thermochimica Acta **419**, 135-141 (2004)

[7] Metglas Inc., *Magnetic Alloy 2826MB (nickel-based) Technical Bulletin* (Metglas Inc., 2011) 1

[8] R.J.J. Martis, T.J. Taylor and Y.P. Khanna, Journal of Non-Crystalline Solids **94**, 209-215 (1987)

[9] Metglas Inc., *https://metglas.com/frequently-asked-questions/\#question_twentyeight* (Metglas Inc., 2017)

[10] E. Palik (edited by), *Handbook of optical constants of solids II* (Academic Press, Inc, 1991)

[11] R. Choithrani, Invertis Journal of Science and Technology **7**, 72-77 (2014)

[12] A. van Roekeghem, J. Carrete, C. Oses, S. Curtarolo, N. Mingo, Physical Review X **6**, 041061 (2016)

[13] D.R. Lide, *CRC Handbook of Chemistry and Physics, 89th Edition (Internet Version 2009)* (CRC Press/Taylor and Francis, 2009) 4-51